Chapter 13
Thiacalixarenes

Nobuhiko Iki

13.1 Introduction

13.1.1 In the Beginning Was Thiacalixarene

Chemists dream of creating new compounds with original molecular motifs and contributing to the long history of evolution, which started with the big bang, followed by the evolution in elementary particles, elements, molecules, life, and then, artificial molecules. If any compound is truly useful for humankind, it will co-exist with humans forever. Calixarene is one such motif, which provides opportunities for versatile modifications leading to useful functions as already described in the previous chapters of this book. During the development of this area, some chemists had wondered about replacing the bridging methylene groups with heteroatoms like sulfur. These thoughts remained in their imagination. The first synthesis was reported by Prof. Sone, who connected *p-tert*-butylphenol with sulfur in a stepwise manner followed by cyclization to afford *p-tert*-butylthiacalix[4]arene (TC4A, with Y. 1.6 %) [1]. The synthesis was laborious and hindered the exploratory study on the function. In the meanwhile, Prof. Miyano was consulted by a company, COSMO Research Institute, about an additive for lubricants used in the internal-combustion engine. He noticed a slightly intense peak, corresponding to the cyclic tetramer of alkylphenol linked by sulfur, in a mass spectrum of a fraction from preparative chromatography of the reaction product. Later, they optimized the reaction conditions and established the one-step protocol to synthesize TC4A (Y. 54 %) [2]. This was the beginning. They did not design nor intend to obtain the molecule or even expect its profuse functions surpassing conventional

N. Iki (✉)
Graduate School of Environmental Studies, Tohoku University, 6-6-07 Aramaki-Aoba, Aoba-ku, Sendai 980-8579, Japan
e-mail: iki@tohoku.ac.jp

P. Neri et al. (eds.), *Calixarenes and Beyond*, DOI 10.1007/978-3-319-31867-7_13

calixarenes as described in this chapter. Interestingly, thiacalixarene was discovered in the industrial field rather than in academia as exemplified by the discovery of "classical" calixarene [3]. The advent of thiacalixarene immediately caught the attention of chemists, who always dream of new chemical functions. Since then, a large number of thiacalixarene research papers have been published [4–10]. In this review, we focus on research that wisely utilizes the bridging sulfur (including sulfinyl and sulfonyl) to derive novel structure, property, reactivity, and function. The author strongly believes that the originality in thiacalixarene research comes from the sulfur. Studies that routinely apply the same chemistry already established for calixarenes, such as modifications of the phenol oxygen and using it, for example, as a ligand for metal ions, are omitted from this review. Dealing with thiacalixarene, chemists should keep in mind whether the chemical function could be achieved with the conventional calixarene or not.

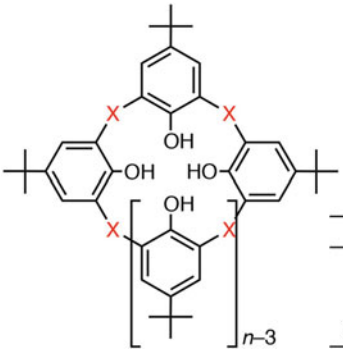

	X	n
TC*n*A	S	4–8
C*n*A	CH_2	4–8
SOCA	SO	4
SO_2CA	SO_2	4

13.2 Covalent Strategy

13.2.1 Synthesis

Before diving into the vast expanse of functions of sulfur-bridged calixarenes, the marked progress achieved in the covalent bond formation in this area should be dealt with. The difficulties encountered in the synthesis of extended thiacalixarenes such as TC6A and TC8A have been rather frustrating and hinder the exploration of their expected functions. Rare thiacalixarenes like TC6A exhibit interesting functions such as inclusion [11, 12], complex formation [13, 14], and metal-clustering ability [15, 16]. In the base-catalyzed oligomerization/cyclization of *p-tert*-butylphenol, TC4A is the predominant species in the presence of NaOH [2, 17]. In a strategy designed to utilize the template effects of alkali metal cations previously observed in the synthesis of *p-tert*-butylcalix[*n*]arene (C*n*A), CsOH was employed for the synthesis of thiacalix[6]arene, but unfortunately, the reaction gave a complex mixture of linear oligomers with a very small amount of TC6A (isolated Y. 0.8 %) [12]. This result suggests that the template effect by cations is not very

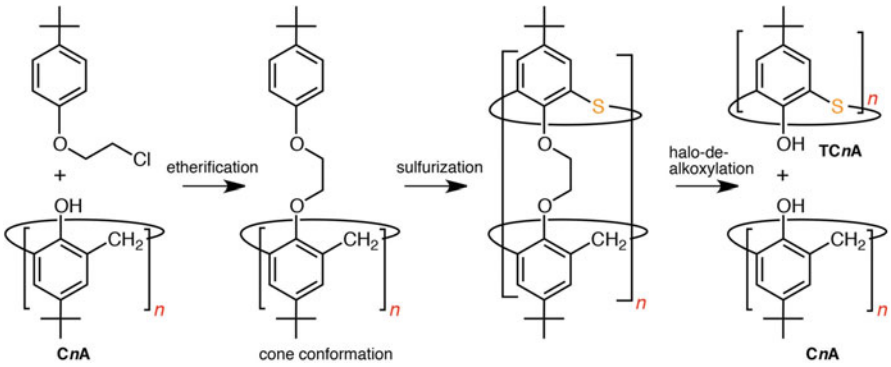

Scheme 13.1 Calix[*n*]arene-templated synthesis of thiacalix[*n*]arene ($n = 4$–8)

effective in the case of TC*n*A. Recently, Patel et al. employed a new strategy based on the principles of pre-organization for the synthesis of these thiacalixarenes (Scheme 13.1) [18]. Here, the individual phenol units are covalently attached to C*n*A ($n = 4$–8) in the required geometry, which are then joined together by sulfur bridges to form the TC*n*A skeleton. Although additional steps such as the removal and separation of the ether tethers and C*n*A are required, the method provides TC*n*A in good yields especially the thiacalixarenes with odd *n* values (38, 32, 23, and 8 % for $n = 5$, 6, 7, and 8, respectively, from C*n*A to the corresponding TC*n*A). An attractive feature of this methodology is that it could be adapted for the synthesis of other types of heteroatom-bridged calix[*n*]arenes. The strategy also tolerates a variety of functional groups on the phenol units. Although there is a lot of scope for further research in the synthesis of thiacalixarenes, these significant developments should open the way for exploring the latent functions of TC*n*A with $n > 4$ as well as of heterocalix[*n*]arenes.

13.2.2 Modification

Modification of TC4A is certainly a direct and useful way to extend the list of functions of these thiacalixarenes. In many cases, the modification methods developed for C4A can be readily adapted to TC4A. However, in this section, we will restrict ourselves to a discussion on the modification methods specific to thiacalixarenes. In some interesting modifications so far, the bridging sulfide has been converted into sulfoxide, sulfone, and sulfimides [7]. A recently reported modification was the *S*-alkylation to a sulfonium moiety, which was attempted by Lhoták et al. [19, 20] Using alkyl triflates as strong alkylating reagents for *O*-propylated TC4As, they succeeded in the preparation of mono- and di-*S*-alkylated thiacalixarenes with controlled regio- and stereoselectivity (Scheme 13.2). These results nicely illustrate the rules governing the alkylation as follows. (i) An

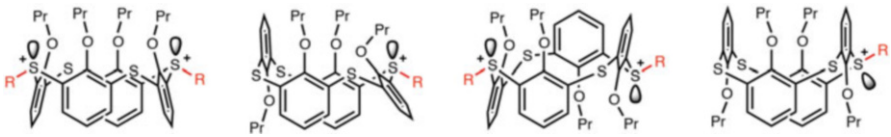

Scheme 13.2 *S*-Alkylated products of tetra(propoxy)thiacalix[4]arene in various conformations

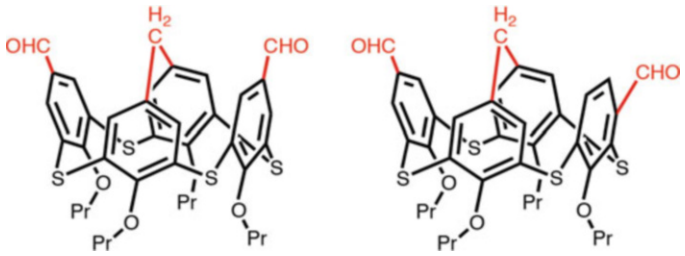

Scheme 13.3 Intramolecularly bridged products of Duff reaction of cone-shaped tetra(propoxy) thiacalix[4]arene

equatorial orientation of the *S*-alkyl group is strongly preferred over the axial. (ii) Proximal sulfur bridges are not alkylated; only distally dialkylated compounds can be formed. (iii) Sulfur connecting phenyl rings in mutually *syn* positions is preferred over one in an *anti* position. (iv) *Anti* position is alkylated only if the molecule does not contain any bridge possessing the *syn* stereochemistry. Consequently, the selectivity seems to be controlled by the steric and electrostatic repulsion in the system. Calixarenes with a cationic moiety in the skeleton would be interesting candidates for anion receptors, in particular for chiral anions, since inherently chiral TC4A could be synthesized by the controlling the configuration of the *S*-alkylated center and the conformation of the *O*-alkylated phenol units.

Chemists have been puzzled by the fact that the reactions used to modify classical calixarenes sometimes cannot be applied to thiacalixarenes seemingly because of the reactivity of the phenol is altered by the sulfur bridges. For example, Lhoták et al. revealed that the formylation [21] and nitration [22] ended up with *meta* rather than *para* substitution in the phenol moiety. Also, during the formylation (Gross and/or Duff conditions) of 1,3-alternate TC4A, two formyl groups were introduced exclusively into the *meta* positions of the thiacalixarene skeleton [23]. DFT calculations revealed that the high electron density at the *meta* position might be responsible for the *meta* substitution. Interestingly, in the case of cone-shaped TC4A, intramolecularly methylene-bridged derivatives (Scheme 13.3) were obtained under Duff conditions. Thus, an interesting interplay between the conformation and the reaction conditions determines the outcome of the formylation reaction of TC4A.

13.3 Molecular Functions

Whether as a host or a ligand, the basic function of the sulfur-bridged calixarenes is the recognition of molecules and ions by inclusion and coordination, respectively. The resulting complexes may then exhibit higher functions, which will be described in the subsequent sections, but herein we focus on recent progress in such molecular functions.

13.3.1 Inclusion

Inclusion is the most fundamental function in host-guest chemistry. As soon as TC4A was synthesized, its inclusion properties were studied in the solid state [1, 17, 24]. Recently, the inclusion of alcohols and carboxylic acid guests into TC4A was studied by Morohashi et al. by suspending the powdery crystals of TC4A in the mixture of the guest liquids [25]. The crystals were suspended in a 1:1 mixture of MeOH-EtOH. After recovering the crystals from the alcohol mixture, the average number (n) of guest molecules bound by TC4A was determined by NMR as $n_{\mathrm{MeOH}} = 0.07$ and $n_{\mathrm{EtOH}} = 0.78$. In the case of EtOH-PrOH the numbers were $n_{\mathrm{EtOH}} = 0.90$ and $n_{\mathrm{PrOH}} = 0.11$. These results suggest a highly selective recognition of EtOH by the TC4A crystals. X-ray diffraction studies of the single crystals of TC4A obtained from each alcoholic solution revealed the hydrogen bonding between the alcoholic and phenolic OH groups and a CH-π interaction between the alkyl and phenyl groups. These interactions resulted in a one-dimensional columnar arrangement of the TC4A molecules in a head-to-tail fashion while connected by the included alcohols (Fig. 13.1). A scrutiny of the distances of the interactions clarified that the EtOH molecules had the strongest interactions with the TC4A, which could be responsible for the high selectivity of the inclusion.

Recently they reported that the inclusion selectivity can be controlled by the conditions such as temperature and polarity of the solvents [26]. For example, from a solution containing 0.43 M Me_2NH and 0.43 M Me_3N in a 1:1 mixture of EtOH/H_2O, Me_2NH was selectively included in the crystals of TC4A (1 M ≡ 1 mol dm^{-3}). On the other hand, Me_3N was selectively included from the solution with the same concentrations of the guests in 1:1 *N*-methylformamide/H_2O. Moreover, they demonstrate a smart method to control the guest inclusion by using a metastable crystal of TC4A instead of the thermodynamically most stable one (Fig. 13.2) [27]. The crystal of TC4A in the most stable form adopting a self-inclusion structure (**1**) was immersed in an aqueous solution of Me_2NH to include the amine as the crystal guest (**2**). The crystal was then suspended in methanol and heated to provide the metastable crystal having a 1D columnar arrangement of TC4A in the head-to-tail manner without any guest molecules (**3**). The metastable crystal exhibited an enhanced ability to include organohalogens from aqueous solutions and switching of the selectivity between HCOOH/EtCOOH by temperature. These results point towards a new strategy to control the inclusion ability and

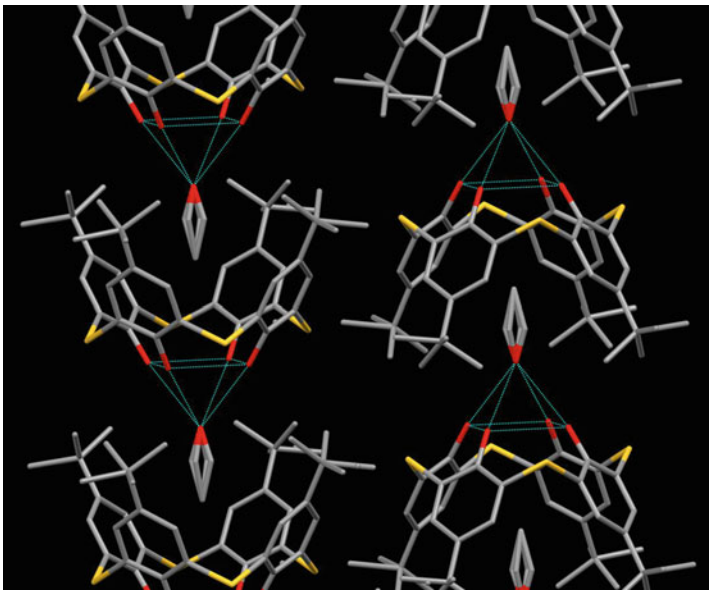

Fig. 13.1 X-ray crystallographic structure of TC4A·EtOH. The *tert*-butyl groups and guest molecules are disordered

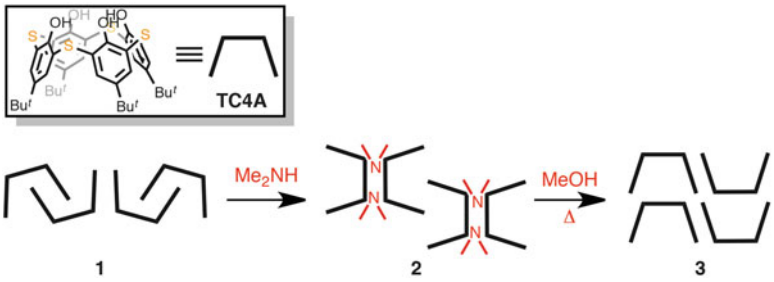

Fig. 13.2 Transformation of thermodynamically stable crystal **1** of TC4A to metastable **3** via **2** including dimethyl amine

selectivity of TC4A by changing the conditions or crystal morphology without modifying the molecule.

13.3.2 Coordination

The most characteristic feature of thiacalixarene is its binding ability towards metal ions by coordination with the bridging sulfur as well as with the adjacent phenol

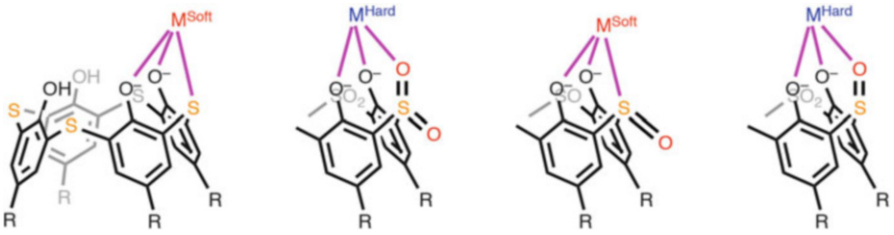

Scheme 13.4 *Exo*-coordination fashion of sulfur-bridged calix[4]arenes. Partial structure is drawn for sulfonyl- and sulfinylcalix[4]arenes

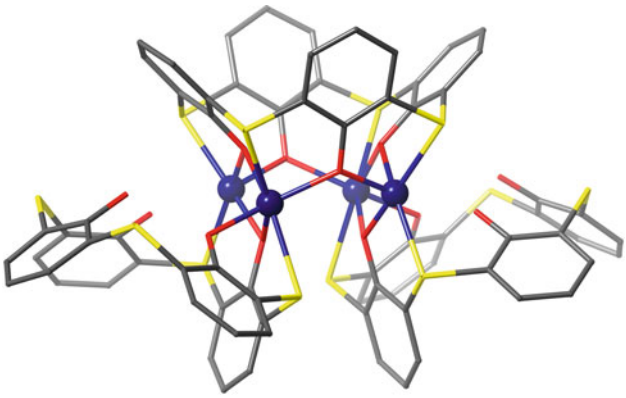

Fig. 13.3 X-ray crystallographic structure of $[Zn^{II}_3(H_2tca)_2(tca)]$. The blue sphere represents Zn^{II} ion. The *tert*-butyl groups are not drawn for clarity

oxygen atoms, i.e., O,S,O *exo*-binding (Scheme 13.4). The striking difference in metal binding in thiacalixarenes compared to the classical calixarene was first revealed by solvent extraction [28]. Besides the binding ability, the selectivity can be controlled by the oxidation states of the bridging sulfur [29]. The thia form prefers so-called soft metal ions to hard ones, but the sulfonylcalix[4]arene prefers the hard metal ions. Interestingly, the sulfinylcalix[4]arene binds to both by switching the ligating atom according to the hardness/softness of the metal ion. The coordination of the bridging sulfur was first revealed for the Zn^{II}-TC4A complex by X-ray diffraction of a single crystal obtained from the organic phase of the solvent extraction of Zn^{II} with TC4A (Fig. 13.3) [30]. Surprisingly, the one of the TC4A ligands assembled Zn^{II}_4 cluster in the crystal to form $[Zn^{II}_4(H_2tca)_2(tca)]$, suggesting that all of the four O,S,O donor sets can accommodate four metal ions at the same time to lead to cluster complexes (H_4tca = TC4A). Later on, a number of crystallographic structures were revealed for sulfur-bridged calixarenes including *p-tert*-butylsulfinylcalix[4]arene (SOCA) and *p-tert*-butylsulfonylcalix[4]arene (SO_2CA), which emphasize their ability to form metal cluster complexes due to the large number of donor atoms present as O_4X_4 (X = S or O) [31, 32]. A systematic

investigation of TC4A-metal complexes was carried out by Harrowfield et al. [33–35] Furthermore, TC6A was revealed to bind to metal ions with selectivity similar to TC4A [14]. In the solid state, TC6A assembled transition metal clusters of Cu^{II}_{10} and Co^{II}_{5}, Ni^{II}_{4}, and $M^{II}Ni^{II}_{4}$ (M^{II} = Mn^{II}, Co^{II}, and Cu^{II}), owing to the O,S,O tridentate fashion [15, 16].

13.4 Supramolecular Functions

As a result of the recognition of molecules and metal ions by calixarene, functions of a higher level (secondary function) than simple binding (primary function) may arise. This can be conveniently described by a mathematical formulation as:

$$f(x+y) > f(x) + f(y) \tag{13.1}$$

where x and y are calixarene and other entities, respectively, and $f(x)$ is the function (of the component x) such as structure, properties, and chemical functions. In other words, the components x and y show a synergistic effect to generate a new function $f(x + y)$. In many cases, however, functionalizing of the calixarene x relies on covalently attaching functional groups y to afford sophisticated molecules $x + y$, which are sometimes referred as supramolecules (super molecule, correctly). As a result, the resulting functions are expressed by Eq. (13.2).

$$f(x+y) = f(x) + f(y) \tag{13.2}$$

On the one hand, this means a success in molecular design where the resulting function $f(x + y)$ is exactly what is expected from $f(x) + f(y)$. For example, when $x =$ calix[4]arene and $y =$ ligating group, then $f(x + y) =$ coordination. On the other hand, this is strictly different from the definition of a supramolecule, because the word "supra" means "*beyond*" and therefore supramolecular function should be greater than what is expected from the individual functions of each components as expressed by Eq. (13.1). Hereafter, truly supramolecular functions defined by Eq. (13.1) such as separation, catalysis, cage formation, magnetism, luminescence, and sensing will be described.

13.4.1 Separation

As mentioned above, the sulfur-bridged calixarenes have been revealed as ligands, and the most direct application of these molecules should be the separation of metal ions. To separate different metal ions, the ligand must be in a medium such as an organic phase or a solid support. The latter is currently preferred from an environmental point of view. Matsumiya used a strong anion-exchange resin as a

convenient support to immobilize thiacalix[4]arene-*p*-tetrasulfonate (TCAS) through the noncovalent electrostatic interaction between the SO_3^- group and trimethylammonium group of the resin [36]. The resulting composite can be used as a chelating resin to separate and preconcentrate metal ions without leaking the TCAS. It can also be applied to the speciation of free Cu^{II} and Cu^{II}-humate in natural water [37]. Hydrophobic interactions can also be used for the noncovalent immobilization. SOCA-impregnated XAD resins can separate Nb(V) from Ta (V) [38]. Furthermore, Kikuchi et al. reported the preparation of SO_2CA-impregnated silica adsorbents for the actinides [39, 40] that showed excellent performance in the separation of trivalent actinides such as Am, from a high-level radioactive liquid waste in a weakly acidic solution. The adsorbent was chemically stable under irradiation and the amount of dissolution of SO_2CA was only 1 % by gamma-ray irradiation at a total dose of 1 MGy. The value of the distribution coefficient of Am at pH 4 by the adsorbent was constant even at the high irradiation dose. Moreover, the separation factor of Am to lanthanides showed a high value. These successes in the separation of metal ions are attributed to the *exo*-binding mode with the O,X,O donor set (X = S or O) present in these molecules and its compatibility with the solid support via a noncovalent immobilization. These characteristic properties of the sulfur-bridged calix[4]arene lead to the emergence of the separation function upon combination with the solid support.

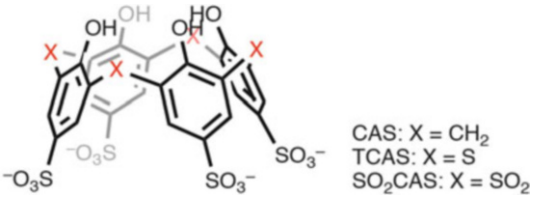

13.4.2 Catalysis

Owing to the controllable Lewis acidity and/or redox potential of the metal center as well as selective binding to a substrate arising from the stereochemistry of ligands, molecular catalysts have been designed based on metal complexes. The *exo*-coordination ability with the O,X,O atoms (X = S or O) to leave the metal center coordinatively unsaturated as well as the ability to assemble a multiple-metal core, the sulfur-bridged calixarenes can provide molecular catalysts with high activity. The first example was a cone-shaped $[Ti^{IV}_2(tca)Cl_4]$ (**4**), which has high catalytic activity in the Mukaiyama-aldol reaction of aromatic aldehydes with silyl enol ethers [41]. Owing to the cone conformation, which brings the two Lewis acid centers to the same sides of the calix, the aldehyde oxygen coordinates to both simultaneously and is activated enough leading to a facile condensation. The

cone-shaped **4** can also be used as a catalyst for the regioselective [2 + 2 + 2] cycloaddition of terminal alkynes [42] and to the polymerization of ethylene [43].

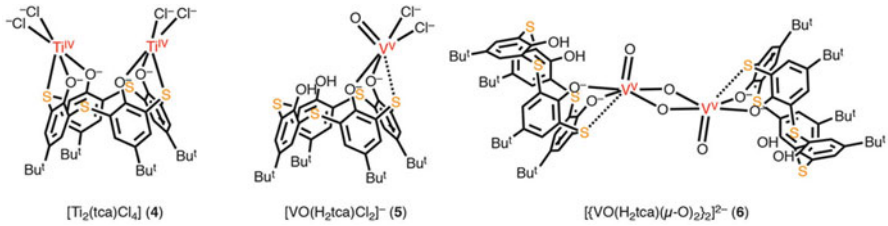

As has been reported, a classical calixarene forms a complex with metal ions with high valency by the coordination of the phenolic O^- group [44]. A wide variety of metal complexes showed catalytic activity, where the phenolic O^- of calix behaves as an oxosurface [45]. For example, the oxovanadium(V)-C4A complex can catalyze the oxidation of alcohols and the polymerization/copolymerization of olefins [46]. Seeking higher catalytic activity, Hoppe et al. prepared mono- and dinuclear oxovanadium(V)-TC4A complexes $PPh_4[VO(H_2tca)Cl_2]$ (**5**) and $(PPh_4)_2[(VO(H_2tca)(\mu\text{-}O))_2]$ (**6**) and assessed their activity to catalyze the oxidation of alcohols with O_2 at 80 °C. X-ray analyses confirmed the *exo*-O,S,O coordination to the V(V) center in both **5** and **6**. The latter showed a somewhat weaker S–V interaction as judged by the distance (2.9446(11) Å) as compared to the one in **5** (2.7553(16) Å). Both **5** and **6** efficiently catalyze the oxidation of benzyl alcohol, crotyl alcohol, 1-phenyl-1-propanol, and fluorenol with turnover frequencies up to 83 h^{-1}. In most cases, the dinuclear complex **6** is more active than the mononuclear complex **5**. Interestingly, the thiacalixarene complexes **5** and **6** are in many instances more active than oxovanadium(V) complexes containing "classical" calixarene ligands. Although a detailed mechanistic study of the observed higher catalytic activity is still awaited, the authors suspect that the acceleration of the rate-determining step (probably the alcohol conversion) is due to the electronic effect of the bridging sulfur.

Thus, taking advantage of the peculiar coordination fashion of TC4A, some success in the application of these molecules as catalysts has been achieved. However, it seems that the development of molecular catalysts of this class is still in its infancy, which may be due to the difficulty in the prediction of catalytic function as shown by Eq. (13.1). Therefore, the rational design of catalysts based on these molecules is still a challenge for chemists who have to rely on empirical studies on structure-activity relationships.

13.4.3 Cage Formation

Owing to the structural beauty and latent functions based on magnetism and luminescence, cluster complexes with high nuclearity is one of the active areas of

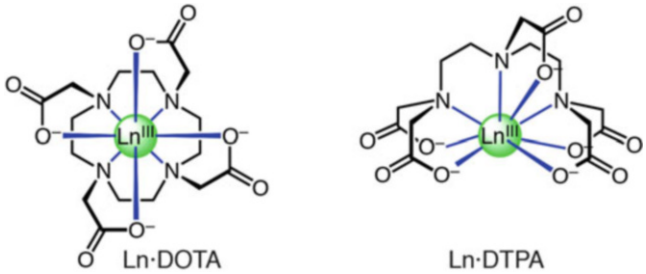

Scheme 13.5 *Endo*-coordination fashion of DOTA and DTPA to lanthanide

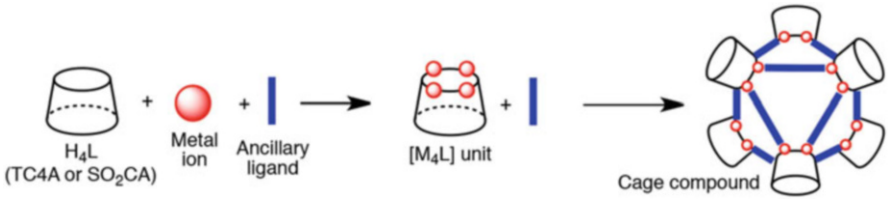

Scheme 13.6 Self-assembly of sulfur-bridged calix[4]arene with a metal ion and ancillary ligand to a cage compound via the tetranuclear unit [M_4L]

research in coordination chemistry. It is a common tactic to design ligands having a large number of donor atoms to accommodate multimetal cores, because use of an excess amount of ligands having low denticity tends to end up forming mononuclear complexes. Another factor, which affects the nuclearity, is the stereochemistry of the ligating atoms to array several metal cores. Even when the denticity is high as in the cases of DOTA and DTPA with 8 donor atoms, they encapsulate a single metal ion inside the molecule (i.e. *endo*-coordination, see Scheme 13.5, DOTA = 1,4,7,10-tetraazacyclododecane-*N*,*N*′,*N*″,*N*‴-tetraacetic acid and DTPA = 1,1,4,7,7-diethylenetriamine pentaacetic acid). As described above, early studies have revealed that the sulfur-bridged calixarenes per se behave as the cluster forming ligands owing to the large number of donating atoms and the *exo*-binding fashion. However, the presence of ancillary ligands and their effects had been greatly unknown. The recent explosive growth in the exploration of giant cage-type complexes with sulfur-bridged calix[4]arenes mainly led by Chinese groups is noteworthy. They focus on molecular cages by assembling the calixarene complexes. The strategy is to react a sulfur-bridged calix[4]arene (H_4L) and a metal salt in the presence of an ancillary ligand under solvothermal conditions (Scheme 13.6). The calix assembles four transition metal ions (M^{x+}) to form M_4L subunits, which are bridged by the ancillary ligand to form a wide variety of cage or polyhedral structures. The variety of the 3D-structures of the cage-shaped complexes can be regarded as the results of supramolecularity between the calix, metal, and ancillary ligand as expressed by Eq. (13.1).

For instance, Su et al. reported the synthesis of coordination cages with high-nuclearity (M_{4n} where M = Ni or Co; $n = 2$–6) using inorganic phosphate or

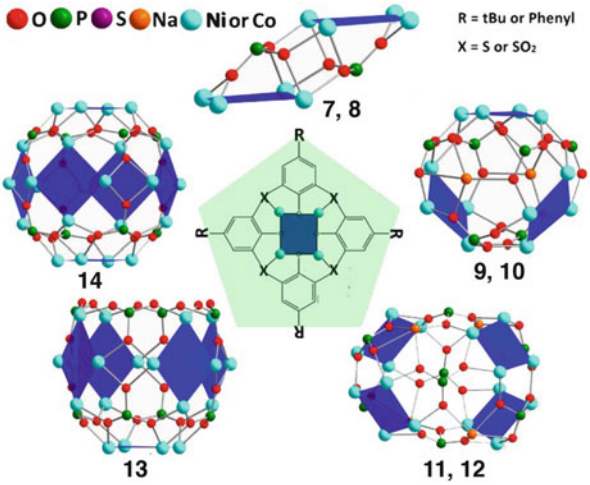

Fig. 13.4 Coordination cages **7–14** obtained from sulfur-bridged calix[4] arenes, M^{II}, and ancillary phosphate ligands (© 2014 American Chemical Society)

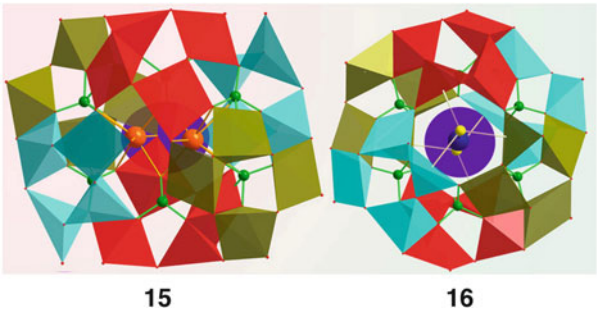

Fig. 13.5 Coordination cages **15** and **16** obtained from TC4A, Co^{II}, and alkali hydrogen phosphates. *Polyhedron*: Co, *green sphere*: P, *orange*: Na, *blue*: K, *yellow*: Cl (© 2014 American Chemical Society)

organic phosphonate ligands as the ancillary ligands [47]. Varying the calix ligand (TC4A, *p*-phenylthiacalix[4]arenes (PTCA), and SO_2CA) and the metal:calix: ancillary ligand ratio gave five types of clusters (Fig. 13.4). Dimeric clusters **7** and **8** ($n = 2$) have a Ni_8 core, which was arranged in a chair conformation. The clusters with sphere-shaped M_{12} (M = Ni(**9**) and Co(**10**), $n = 3$) and capsule-like M_{16} (M = Ni(**11**) and Co(**12**), $n = 4$) have closed-shell structures, where their ports are sealed by sodium ions. The helmet-like Co_{20} (**13**) is the only one in this family with an open-shell structure, which can be regarded as a truncated octahedral Co_{24} (**14**) nanocage cutting one face.

More recently two kinds of coordination cages including alkali metal ions were formed by the solvothermal reaction of TC4A, $Co(NO_3)_3$, and Na_2HPO_4/K_2HPO_4 in DMF-MeOH (Fig. 13.5) [48]. On one hand, the disodium salt gave the oval-shaped capsule, $[Na_2Co_{24}(tca)_6(PO_4)_6(HCOO)_6(DMC)_2(DMF)_2(dma)_4]$ (**15**), inside which two sodium ions were included (DMC = *N*,*N*′-dimethylcarbamate, dma = dimethylamine). The capsule was capped by six $[Co_4(tca)]^{4+}$ units and six phosphate linkers and other different auxiliary anions, possessing a Co_{24} core

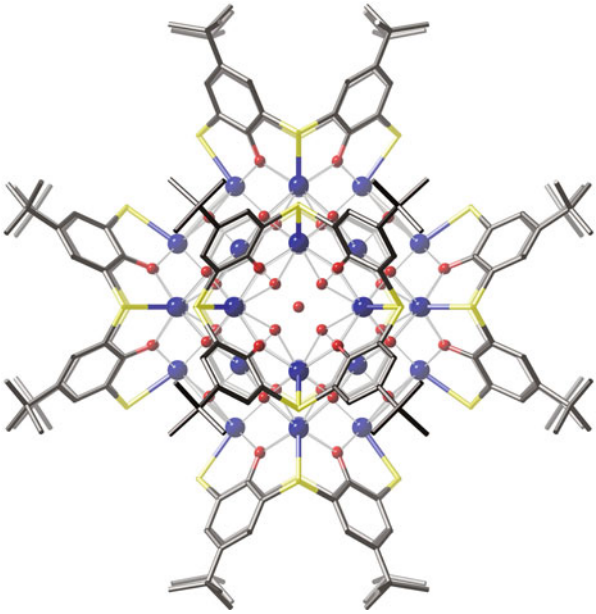

Fig. 13.6 X-ray crystallographic structure of coordination cage $[Co^{II}_{24}Co^{III}_{8}(\mu_3\text{-}O)_{24}(H_2O)_{24}(tca)_6]$. *Blue sphere*: $Co^{II/III}$ ion

templated by two Na^+ ions. On the other hand, a dipotassium salt gave spherical cages of cationic $[KCo_{24}(tca)_6(PO_4)_6Cl_2(HCOO)_4(DMF)_8]^+$ (**16**) and anionic $[KCo_{24}(tca)_6(PO_4)_6Cl_2(HCOO)_6(DMF)_4(CH_3OH)_2]^-$, sharing the same subunits with **15** but including only one K^+ ion in each capsule.

In terms of nuclearity, the highest reported so far is M_{32} clusters. The first example was a giant spherical cage, $[Co^{II}_{24}Co^{III}_{8}(\mu_3\text{-}O)_{24}(H_2O)_{24}(tca)_6]$, prepared by the solvothermal reaction of $Co(AcO)_2$ and TC4A in a 1:1 mixture of MeOH/$CHCl_3$ (Fig. 13.6) [49]. The $[Co^{III}O_6]_8$ cube was formed in situ to act as an ancillary ligand and bridged six $[Co^{II}_4(tca)]^{4+}$ units located at the vertices of the octahedron to form a giant sphere. The peripheral diameter defined by the distance between two *tert*-butyl carbons of two distal TC4A molecules on the sphere was about 2.3 nm. In addition, the diameter of the inner cavity was estimated to be 4.8 Å. Other examples reported so far are $[Ni^{II}_{32}(OH)_{40}(tca)_6]$ [35] and $[M^{II}_{32}O_{16}(OH)_8(CH_3OH)_6(tca)_6]$ (M = Co, Ni) [50], which were prepared by a reaction between the metal salts and TC4A in DMF at room temperature. These share a few common features such as bridging of the six $[M_4tca]^{4+}$ units by eight MO_6 units and the resulting giant spherical form. Surprisingly, such highly ordered molecular edifices were readily constructed by simply mixing the components under solvothermal or nonsolvothermal conditions, suggesting that the $[M_4tca]^{4+}$ cluster units seemingly sought a bridging MO_6 unit to assemble together to form the giant sphere.

Using high-valence oxometalates as ancillary components, heterometallic cluster complexes can be formed by a one-step synthesis. The solvothermal reaction of $Co(OAc)_2$, TC4A, and $Na_2M^{VI}O_4$ in EtOH/$CHCl_3$ readily afforded

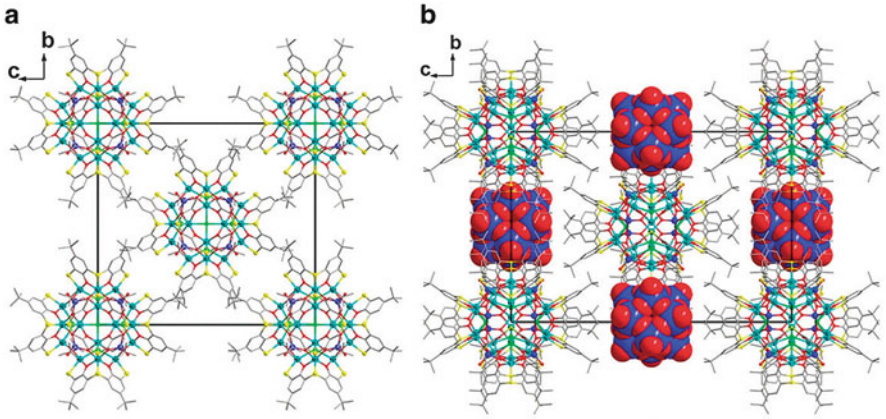

Fig. 13.7 Packing diagrams of (**a**) $[Co_{24}(tca)_6(MoO_4)_8Cl_6](OH)_2(CHCl_3)_{12}(CH_3CH_2OH)_{12}$ and (**b**) $[Co_{24}(tca)_6(MoO_4)_8Cl_6][HPM_{12}O_{40}](CHCl_3)_{12}(CH_3CH_2OH)_7$ (© 2011 Royal Society of Chemistry)

$[Co_{24}(tca)_6(MO_4)_8Cl_6]^{2+}$ (M = Mo or W, Fig. 13.7a) [51]. It has a spherical shape with a diameter being of *ca*. 2.3 nm, which is quite similar to that observed in the $[Co^{II}{}_{24}Co^{III}{}_8(\mu_3\text{-}O)_{24}(H_2O)_{24}(tca)_6]$ nanosphere except that the $[Co^{III}O_6]$ sites have been replaced by the $[MO_4]$ groups and the water molecules in the lower rim of the $[Co_4tca]^{4+}$ units have been substituted by the Cl^- anions. The cubic $(MO_4)_8$ assemblies in the cationic nanospheres penetrate through the $Co^{II}{}_{24}$ sodalite cages while the $Co^{III}{}_8$ cube in the $[Co_{32}]$ nanosphere is located inside the sodalite cage. Interestingly, in the case using $H_3PM_{12}O_{40}$ as the ancillary component, the cationic nanosphere formed hybrids with Keggin polyoxyometalates $[HPM_{12}O_{40}]^{2-}$ to result in a superstructure in which $[HPM_{12}O_{40}]^{2-}$ is surrounded by six nanospheres occupying the vertices of an octahedron (Fig. 13.7b). The success of this method relies on the complexation selectivity of TC4A, which does not react with Mo^{VI} and W^{VI}.

Organic ligands can also serve as the ancillary bridging ligand. Liao et al. used aromatic di- or tricarboxylic acids, bifunctional carboxylic acids, and azoles as the ancillary ligands to bridge the M_4L units (H_4L = TC4A or SO_2CA) [52]. Clusters of octahedral cage $[(M_4L)_6(tc)_8]$ (tc = aromatic tricarboxylates), octahedral cage $[(M_4L)_6(dc)_{12}]$, square $[(M_4L)_4(dc)_8]$, tetragonal $[(M_4L)_4(dc)_4]$ (dc = aromatic dicarboxylates), wheel $[(M_4L)_6(trz)_{12}]$ (trz = 1,2,4-triazole) [53], wheel $[(M_4L)_4(tta)_8]$ (tta = 5-Me-tetrazolate) [54], and tetragonal prismatic $[(M_4L)_8(btz)_4(N_3)_8]$ (btz = 1,3-bis(2H-tetrazol-5-yl)benzene) [55] were constructed. More recently, an extra-large octahedral coordination cage (overall peripheral diameter of 5.4 nm and an internal cavity of 2.7 nm) was prepared with $[Co_4(so_2ca)]^{4+}$ units ($H_4(so_2ca) = SO_2CA$) and extended tricarboxylate, 4,4′,4″-(benzene-1,3,5-triyl-tris(benzene-4,1-diyl))tribenzoate ligands [56]. In addition, the same modular approach by using $[M_4(so_2ca)]^{2+}$ and di- and tricarboxylates has been reported by Wang et al. [57–59].

Although these systematic studies have demonstrated the usefulness of the combination of the components such as metal, calix, and the additional ligand in the construction of the large cluster cages, they also have indicated some limitations of the resulting cluster systems. Firstly, the rational design of these cages is still difficult because the outcome of the components are often affected by the in situ generated ligand such as MO_6, tri- and tetrazole or even Cl^- from the $CHCl_3$ solvent. Secondly, the physicochemical properties and functional characteristics of the giant cages still need to be uncovered. For example, the magnetic properties of these cages were often studied but they only show the properties of the $[M_4L]^{x+}$ units, which is typically the antiferromagnetic coupling between the metal centers. Finally, the giant space created by the assembly of $[M_4L]^{x+}$ units cannot be accessed from outside because of the closed structure of these cages. These are significant weaknesses compared to metal-organic frameworks and cluster complexes with other types of ligands. Nonetheless, the beauty of the resulting structures should provide enough motivation to calixarene chemists for pursuing studies on these cages.

13.4.4 Magnetism

One of the characteristic properties of the metal complexes is the molecular magnetism depending on the number of unpaired electrons at the metal center. Recently, single molecule magnets (SMMs), which exhibit superparamagnetic behavior below a blocking temperature, have attracted a lot of attention for applications in memory devices with high density. The magnetic properties of the complexes of thia- and sulfonyl calixarenes with 3d and 4f transition metal ions have been investigated. In some cases, SMM behavior can be found. In an early example, Kajiwara et al., reported that di-Tb^{III} complex of SO_2CA shows superparamagnetic behavior due to the slow magnetic relaxation at low temperatures [60]. They took advantage of Tb^{III} having a large angular momentum and strong magnetic anisotropy in the ground multiplet state. In addition, the SO_2CA has *exo*-O,O,O donor sets with negative charges in a narrow area to stabilize the ground sublevel, which leads to a strong easy-axis anisotropy. The results of these studies suggest that the sulfur-bridged calixarenes can be a platform to obtain SMMs. Using PTCA (H_4ptca), Bi et al. solvothermally synthesized $[Dy^{III}{}_4(ptca)_2(\mu_4\text{-OH})Cl_3(CH_3OH)_2(H_2O)_3]$, which showed a slow magnetic relaxation behavior characteristic of SMM behavior [61].

The 3d transition metal ions can also give SMMs. For example, Desroches et al. have studied the magnetic properties of polynuclear complexes of the calixarenes with 3d transition metal ions [62, 63]. Recently, they reported the formation of a series of Co^{II}-SO_2CA complexes by a one-pot solvothermal reaction and succeeded in preparation of a variety of polynuclear complexes: three dinuclear $[Co^{II}{}_2(so_2ca)X_n]$ in 1,2-alternate form (X_n = py_4, bpy_2, or en_2), $[Co^{II}{}_{14}(so_2ca)_3(\mu_4\text{-OH})_3(\mu_6\text{-O})_3(OCH_3)_6]^+[Co^{II}{}_4(so_2ca)_2(\mu_4\text{-OH})]^-$ cluster salt, and

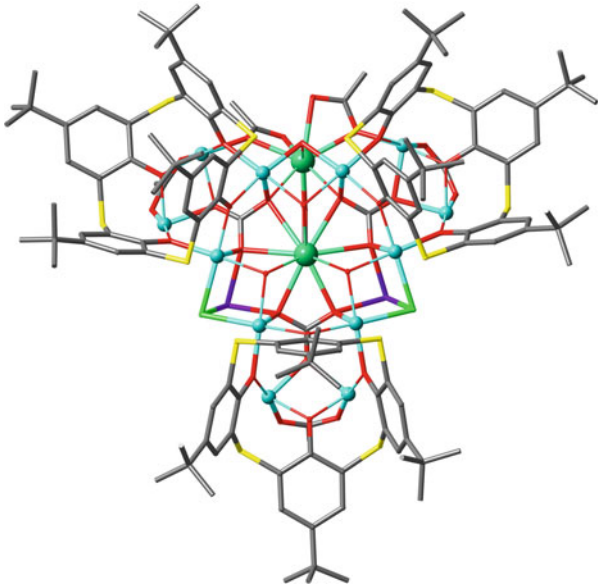

Fig. 13.8 X-ray crystallographic structure of heterometallic cluster $[Na_2Ni^{II}{}_{12}Tb^{III}{}_2(tca)_3(\mu_7\text{-}CO_3)_3(\mu_3\text{-}OH)_4(\mu_3\text{-}Cl)_2(OAc)_6(dma)_4]^{2+}$. *Dark green*: Tb^{III}, *light blue*: Ni^{II}, *purple*: Na^{I}

tetranuclear $[Co^{II}{}_4(so_2ca)_2(\mu_3\text{-}OH_2)]$ cluster [64]. The addition of the chelating ligands X was shown to be a critical factor to stabilize the dinuclear complexes $[Co^{II}{}_2(so_2ca)bpy_2]$ and $[Co^{II}{}_2(so_2ca)en_2]$, which showed slow relaxation of magnetization at small magnetic fields.

Introducing both 3d and 4f elements in the molecule is another way to design SMMs. In thiacalixarene territory, Xiong et al. reported the preparation of the heterometallic cluster $[Na_2Ni^{II}{}_{12}Ln^{III}{}_2(tca)_3(\mu_7\text{-}CO_3)_3(\mu_3\text{-}OH)_4(\mu_3\text{-}Cl)_2(OAc)_6(dma)_4]^{2+}$ (Ln = Dy or Tb, dma = dimethylamine, Fig. 13.8) [65]. In the complex, three $[Ni^{II}{}_4tca]^{4+}$ units are linked together in an up-to-up fashion through two Na^+ ions and two Ln^{III} ions, along with other anions, leading to a pseudo-trigonal planar entity. Within this entity, there is a trinary-cubane core composed of one $[Ni_2Ln_2]$ cubane unit and two $[NaNi_2Ln]$ cubane units sharing a Ln^{III} ion. Magnetic studies reveal that the Dy^{III} complex shows the slow relaxation of the magnetization expected for SMM behavior. Regrettably, however, the cooperativity between the 3d–4f metal ions was not observed. Su et al. reported the synthesis of $[Zn^{II}Ln^{III}{}_3(\mu_4\text{-}OH)(tca)_2(OAc)_2(CH_3OH)(H_2O)(DMA)_2] \cdot 3H_2O$ in which a $Zn^{II}Ln^{III}{}_3$ heterometallic cluster is sandwiched by two cone-shaped TC4A ligands (Ln = Gd, Tb, Dy, Ho, DMA = *N*,*N*′-dimethylacetamide) [66]. Some antiferromagnetic interactions between the Ln^{III} ions are observed in the complexes. The *ac* susceptibility measurement on the Dy^{III} complex reveals an obvious frequency-dependent in- and out-of-phase signal, indicating the slow magnetization relaxation typical for SMMs. Thus, the quest for thiacalix-based SMMs having higher blocking temperatures and also reducing the probability of quantum tunneling is still on.

13.4.5 Luminescence

Molecular-based luminescence materials are used in luminescent display devices, inks, and bio-analysis and imaging [67–70]. Because the calixarenes are not fluorescent, they cannot be used as luminescent materials without introducing a luminescent center. Introducing a fluorophore is not ideal unless the calix part plays an essential role in the fluorescent function. A more rational approach is to introduce a luminescent metal center such as a lanthanide(III) ion, which can be excited by energy transfer from the antenna group in the ligand in its T_1 state. Attached with auxiliary ligand(s), classical calixarenes have been proven to be good ligands for the energy-transfer luminescence of Ln^{III} [71]. Here, the calix[4]arene skeleton acts as the platform to attach the ligating group and as a light-absorbing antenna to excite the Ln^{III} center. An auxiliary antenna group should also be introduced if the T_1 state of the calix does not match the excitation of Ln^{III}. By using the inherent coordination ability of the sulfur-bridged calixarenes, we studied the formation of Ln^{III} complexes with water-soluble calixarenes TCAS and sulfonylcalix[4]arene-*p*-tetrasulfonate (SO_2CAS) in aqueous solutions [72]. Among the Ln^{III} species, Tb^{III} exhibited strong luminescence with the calixarenes. TCAS formed a 1:1 complex ($Tb^{III} \cdot$ TCAS, Scheme 13.7) at pH $\geq$ 8.5, exhibiting the Tb^{III}-centered luminescence with a quantum yield $\Phi = 0.15$ and a lifetime $\tau = 0.71$ ms. Reflecting the high acidity of the ligand [73], the sulfonyl counterpart ($Tb^{III} \cdot SO_2CAS$) at pH ≥ 5.5 also showed luminescence ($\Phi = 0.13$, $\tau = 0.70$ ms). By contrast the classical calixarene, calix[4]arene-*p*-tetrasulfonate (CAS), formed a 1:2 luminescence complex, $Tb^{III} \cdot CAS_2$, at very high pH (pH > 12, $\Phi = 0.12$, $\tau = 0.61$ ms), indicating that the coordination only by the phenol oxygen is very weak in aqueous solution. These results endorse the usefulness of the sulfur-bridged calixarenes in terms of formation of the luminescent Tb^{III} complex, owing to the inherent *exo*-coordination ability of the ligand and the T_1 level suitable for the excitation.

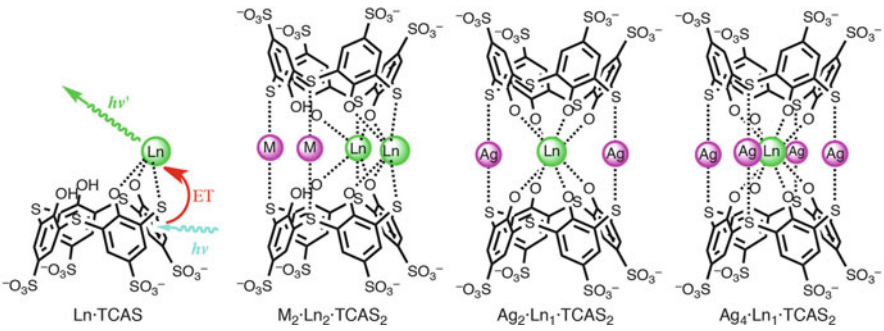

Scheme 13.7 Structures of the Ln^{III}-TCAS complexes. For Ln·TCAS, energy-transfer luminescence is schematically drawn

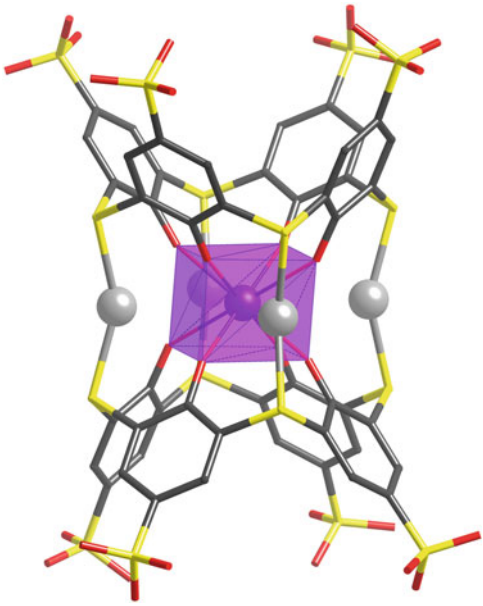

Fig. 13.9 X-ray crystallographic structure of $Ag^{I}_{4}{\cdot}Tb^{III}{\cdot}TCAS_2$. Chemical formula: $Na_9[Ag_4Tb(tcas)_2dmf_2](dmf)_6(H_2O)_6$ (H_4tcas^{4-} = TCAS). The purple cube depicts the O_8-cubic coordination geometry of Tb^{III} provided by two TCAS ligands

During efforts to study the effect of diverse ions coexisting in the solution on the luminescence intensity of Tb^{III} · TCAS, Horiuchi unexpectedly found that Ag^{I} enhanced the luminescence intensity. The scrutiny of the Ag^{I}-Tb^{III}-TCAS system by electrospray ionization mass spectrometry (ESI-MS) and molar ratio methods clarified that at pH 6 a ternary complex $Ag^{I}_{2}{\cdot}Tb^{III}_{2}{\cdot}TCAS_2$, was formed [74]. Moreover, in the presence of excess amount of Ag^{I} and TCAS to Tb^{III} at pH 10, $Ag^{I}_{2}{\cdot}Tb^{III}{\cdot}TCAS_2$ formed as the main luminescent species. The structures of $Ag^{I}_{2}{\cdot}Tb^{III}_{2}{\cdot}TCAS_2$ and $Ag^{I}_{2}{\cdot}Tb^{III}{\cdot}TCAS_2$ was proposed on the basis of the crystal structure of $Ag^{I}_{4}{\cdot}Tb^{III}{\cdot}TCAS_2$ (Fig. 13.9), in which two TCAS ligands are linked by four S–Ag(I)–S linkages [75]. Among the photophysical properties, the exceptionally long-lived luminescence of $Ag^{I}_{2}{\cdot}Tb^{III}{\cdot}TCAS_2$ (4.6 ms) should be noted, which could be due to the O_8-cubic coordination environment provided to Tb^{III} to expel coordinating water from Tb^{III}. In fact, the number of coordinating water molecules to Tb^{III} was estimated to be 0.1 using Horrocks' equation. Taking advantage of the O_8 coordination environment of Tb^{III} provided by $Ag^{I}_{4}{\cdot}Tb^{III}{\cdot}TCAS_2$, the analogous Nd^{III} complex $Ag^{I}_{4}{\cdot}Nd^{III}{\cdot}TCAS_2$ was formed via self-assembly [76]. This complex exhibited efficient near infrared (NIR) luminescence ($\Phi = 4.8 \times 10^{-4}$) even in water, which is usually a strong quencher of the excited states of Nd^{III} via the coupling to the overtone of the O–H vibration. The Ag^{I}-Ln^{III}-TCAS system provides a good example of the supramolecularity: the resulting structure and function (such as the O_8-cubic coordination geometry, the long-lived luminescence of Tb^{III}, and efficient NIR luminescence of Nd^{III}) are beyond that predicted from the individual properties of each component (Eq. (13.1)). Among the components, the most valuable player is undoubtedly

TCAS, which selectively provides the S and O donor atoms to the ions in the complexes $Ag^{I}_2{\cdot}Tb^{III}{\cdot}TCAS_2$ and $Ag^{I}_4{\cdot}Ln^{III}{\cdot}TCAS_2$.

Besides Ag^{I}, other metal species that form luminescent ternary complexes with Tb^{III} and TCAS were examined [77]. Among Fe^{III}, Ni^{II}, Zn^{II}, Pd^{II}, Cd^{II}, Hg^{II}, Tl^{I}, and Pb^{II}, only Cd^{II} gave more intense luminescence than a Tb^{III}-TCAS binary system. The luminescence occurs at a pH around 6.5 with the formation of a ternary complex. The ESI-MS results revealed that the species formed at pH 6.5 was $Cd^{II}_2{\cdot}Tb^{III}_2{\cdot}TCAS_2$ ($\Phi = 0.15$, $\tau = 1.12$ ms, very similar to the case of $Ag^{I}_2{\cdot}Tb^{III}_2{\cdot}TCAS_2$). However, the Cd^{II} system did not form the 2:1:2 ternary complexes like $Ag^{I}_2{\cdot}Tb^{III}{\cdot}TCAS_2$ at higher pH values. This is because the S–Cd^{II}–S linkages are shorter than S–Ag^{I}–S, which brings the two TCAS ligands closer together and ejects Tb^{III} from the center of the complex. These results suggest that the formation of the ternary complex relies on precise recognition of ionic radii of Ln^{III} and Ag^{I}/Cd^{II} by the TCAS ligand.

One of the potential applications of the luminescence complexes is in molecular probes for bio-imaging and bio-analysis [78]. A large luminescence quantum yield and long lifetime are desirable for the sake of highly sensitive and time-resolved detection with a high signal-to-background ratio. Another indispensable property is the kinetic stability, because the probes are used in a situation where the free components (ligand and metal ion) are removed. To obtain high kinetic stability, ligands with high denticity to encapsulate Ln^{III} inside the molecule by *endo*-coordination fashion are used as exemplified by DOTA and DTPA (Scheme 13.5). Quite recently, we noticed a gradual change in the absorption spectra of Ln^{III}-TCAS binary systems. The monitoring of the aqueous mixture of TCAS and Ln^{III} (= Nd^{III} or Yb^{III}) with HPLC revealed that the composition changes from $Ln^{III}{\cdot}TCAS$ to $Ln^{III}_3{\cdot}TCAS_2$ occur to form a cluster-type complex over a long period of time (1 d) [79]. Because of the Ln^{III}_3 core sandwiched between the two TCAS ligands, the $Ln^{III}_3TCAS_2$ complex is not only luminescent but also kinetically stable. For example, the observed dissociation rate constant of $Yb^{III}_3{\cdot}TCAS_2$ is 1.26×10^{-4} s^{-1} (25 °C, at pH 1.16), which corresponds to the $t_{1/2}$ value of 1.53 h. This was not expected from the *exo*-coordination fashion of TCAS with the O,S,O donors found in $Ln^{III}{\cdot}TCAS$, and thus, this feature was attributed to the multiple bonds between the Ln^{III}_3 core and TCAS. Here, the kinetic inertness is another example of supramolecularity of the components, where multidenticity of TCAS plays an essential role. Thus, the $Ln^{III}_3TCAS_2$ complex opens an exciting possibility of designing kinetically stable Ln^{III} complexes by using *exo*-type ligands as scaffolds to sandwich a multi-Ln^{III} core rather than *endo*-type ones to encapsulate a Ln^{III} core. Extensions of the $Ln^{III}_3{\cdot}TCAS_2$ in two directions are now underway. The first is not luminescence probe but the design of a magnetic resonance imaging (MRI) contrast agent ($Gd^{III}_3{\cdot}TCAS_2$) [80]. The second is a heterolanthanide assembly $Tb^{III}_{3-x}{\cdot}Yb^{III}_x{\cdot}TCAS_2$ ($x = 1, 2$) to realize f-f communication between the two different lanthanide centers that will lead to enhanced Yb^{III} luminescence or down-conversion [81].

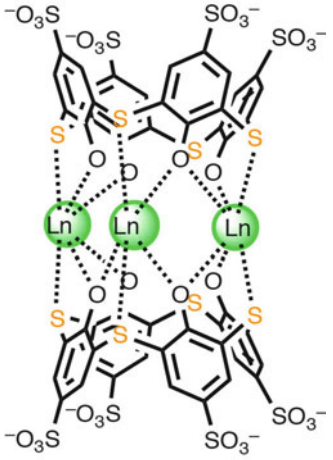

$Ln_3{\cdot}TCAS_2$

13.4.6 Sensing

Sensing has been one of the main applications of calixarenes owing to its facile modification with binding and reporter groups to enable optical or electrochemical signaling [82–86]. Sharing the same phenol moiety, TC4A can be modified and used in the same fashion as exemplified by the literature cited in the recent review [10]. However, such modification without using the bridging sulfur is a typical *mottainai* (wasteful) way of application of TC4A and will not be described here.

Sensing can be divided into two major modes: electrochemical and optical. In the former, an analyte is detected by the electrochemical potential generated at the membrane surface as seen in potentiometry, or by current upon oxidation (or reduction) of the accumulated analyte in the reduced (or oxidized) form as seen in stripping voltammetry. Therefore, in electrochemical sensing, TC4A does not have to be modified with any reporter moiety. For example, TC4A was used as the ionophore for Cu^{II} sensors based on field-effect transistor and electrolyte-insulator-semiconductor sensor. The TC4A was used as thin films (thickness: 20–100 nm) formed by thermal sublimation (10^{-6} Torr, 270–280 °C) [87, 88]. The sensor enabled the detection of Cu^{II} at low (10^{-5} M) levels by the complexation of Cu^{II} with the TC4A layer, which should be due to the coordination ability of the bridging sulfur.

In the voltammetric scheme, Zheng et al. reported the simultaneous determination of Pb^{II} and Cd^{II} by a glassy carbon electrode (GCE) modified with a Langmuir–Blodgett (LB) film of TC4A [89]. In the accumulation step, the TC4A film seemed to form a complex with Pb^{II} and Cd^{II} to preconcentrate these metal ions. After reduction, the metal ions were measured by differential pulse stripping voltammetry, enabling their ultratrace determination with the detection limits

2×10^{-8} M (Cd^{II}) and 8×10^{-9} M (Pb^{II}), respectively. The method can be successfully applied to real samples (river, lake and tap water), where the selectivity of TC4A to the heavy metal ions over other hard metal ions in the samples should play a key role.

Recently, Wang et al. covalently attached TC4A to multiwalled carbon nanotubes (MWCNT) to obtain chemically modified electrodes for anodic stripping voltammetry to detect ultratrace Pb^{II} [90]. The stripping response is highly linear ($R = 0.999$) over a Pb^{II} concentration range of 2×10^{-10} to 1×10^{-8} M, and the limit of detection is 4×10^{-11} M. The improved sensitivity seems to originate from the high surface area and excellent conductivity of the MWCNT.

As can be seen in the electrochemical methods, the analyte itself can act as the reporter. Therefore, it was not necessary for TC4A to be modified with electrochemical reporters. In the case of luminescence sensing for metal ions, the metal ions per se do not usually show luminescence because of the poor ability in the absorption of photon, quenching by solvent, and the forbidden d-d and f-f transition for the luminescence. An easy method to detect metal ions by luminescence is to design a fluorescence sensor having both ion-binding and fluorescent moieties, which was seen in both calix- and thiacalixarene research. There are many examples for thiacalixarenes in which the auxiliary binding moiety nicely binds to metal ions as intended but at the same time the bridging sulfur has no role to play. Combining with reporter materials in a noncovalent fashion, TC4A will behave as the signal-transducing unit by virtue of its intrinsic binding ability towards a metal ion. For example, a quantum dot (QD), which is a nanocolloidal particle of semiconductors, can be a luminescent probe owing to its attractive features such as narrow and tunable emission band, high quantum efficiency, high durability to photobleaching, and broad excitation band. For these reasons, the application of QDs to bioanalytical chemistry is a hot area of research. However, QD per se does not possess the ability to respond to certain analyte ions or molecules. Jin et al. coated CdSe/ZnS quantum dots with 25,26,27,28-tetra(carboxymethoxy)-2,8,14,20-tetrathiacalix[4]arene (TCC) by simply mixing them in THF followed by the deprotonation of TCC with *t*-BuOK (Fig. 13.10) [91]. The coating proceeded

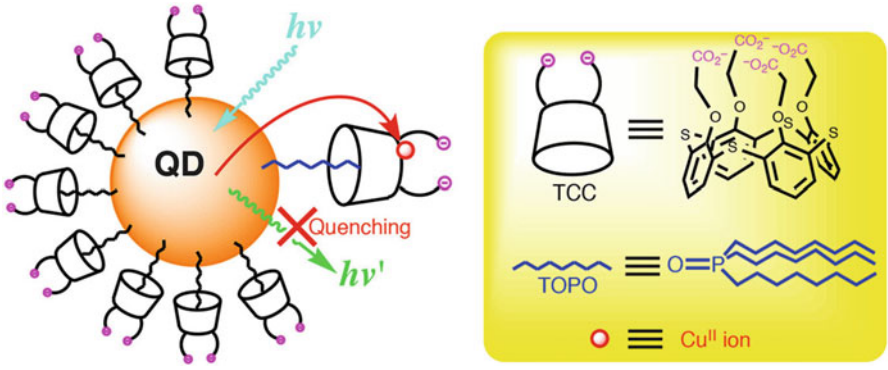

Fig. 13.10 Sensing of Cu^{II} with a QD/TOPO/TCC supramolecular system

by self-assembly of TCC onto trioctylphosphine oxide (TOPO) on the QD via hydrophobic interactions. This converts the QD into a water-soluble supramolecular fluorescent sensor for Cu^{II}, in which the TC4A moiety acts as the signal transducer to bind to Cu^{II} to quench the luminescence of the QD. In the absence of Cu^{II}, the luminescence quantum yield was higher (0.21) than that achieved with QDs surface-modified with mercaptoacetic acid and mercaptoundecanoic acid. The fluorescence of the TCC-coated QDs was selectively quenched by Cu^{II} ions even in the presence of other transition metal ions such as Cd^{II}, Zn^{II}, Co^{II}, Fe^{II}, and Fe^{III} in the same solution. The quenching mechanism followed a static manner, implying that a selective complexation of TCC moiety to Cu^{II} is responsible for the observed selectivity. The fluorescence of TCC-coated QDs was almost insensitive to other physiologically important ions such as Na^{I}, K^{I}, Mg^{II}, and Ca^{II}, suggesting that the TCC-coated QDs can be used as a fluorescent Cu^{II} ion probe for biomedical samples. Here the TCC is the key multifunctional material as the QD coating to make it water soluble, ion-selective ligand, and transducer to quench the luminescence of the QD.

Recently, Hu et al. prepared a Cu^{II}-selective self-assembled fluorescent chemosensor by solubilizing both TC4A as the ion-binding moiety and perylene as the fluorescent reporter in a micelle of a nonionic surfactant Triton X-100 (Fig. 13.11) [92]. Upon addition of Cu^{II} to the micelle solution, the fluorescence emission of perylene inside the micelles was quenched. The authors attributed this to intramicellar electron-transfer or energy-transfer from perylene to Cu^{II}-TC4A complex induced by the complexation of TC4A with Cu^{II} ion. Copper(II) ions can be detected selectively in the presence of other metal ions (Zn^{II}, Pb^{II}, Cd^{II}, Mn^{II}, Ni^{II}, Al^{III}, Na^{I}, K^{I}, Ca^{II}, and Mg^{II}) and its concentration in the submicromolar range can be determined based on the fluorescence quenching. The micelle provides water-solubility to both TC4A and perylene, and confined space to facilitate the complex-fluorophore interaction, where TC4A acted as the signal transducer for Cu^{II}.

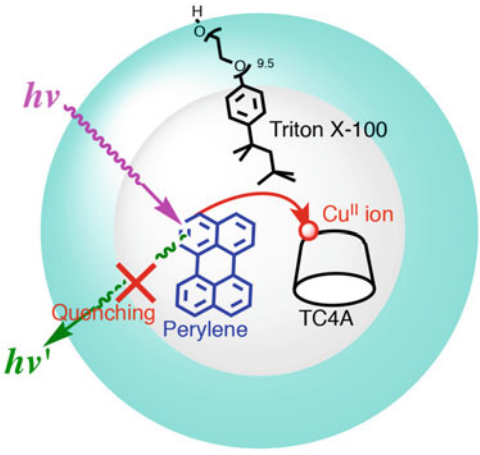

Fig. 13.11 Quenching sensing of Cu^{II} with Triton X-100 micelle containing TC4A and perylene. The *large blue sphere* represents hydrophilic region of the micelle, while white sphere does the hydrophobic core

Since the resulting function of the TC4A-perylene-micelle ternary sensor exceeds the expected individual function from the component, the sensor can be regarded as a supramolecular system.

Metal ions having luminescence function can be used in molecular-based chemosensors without using colloidal materials such as QD and micelles. As mentioned above, Ln^{III} can emit visible to NIR light with high efficiency if the excited energy can be transferred from the T_1 state of an antenna ligand such as TCAS and SO_2CAS [72, 79]. The formation of Tb^{III}·TCAS can be readily applied for the luminescence detection of Tb^{III} at sub-ppb levels [93]. From the viewpoint of multifunctionality of thiacalixarene, Tb^{III}·TCAS still has sites to interact with ions and molecules: the remaining O,S,O binding sites and the hydrophobic cavity.

For the latter, we studied the luminescence quenching of Tb^{III}·TCAS by a cationic guest such as the quaternary ammonium ion [94]. For example, 1-ethylquinolinium quenched the luminescence of Tb^{III}·TCAS most efficiently, affording a very low detection limit (D.L. $= 6.71 \times 10^{-10}$ M, S/N = 3). The agreement of the Stern-Volmer (SV) coefficients obtained with luminescent intensity ($K_{SV,all} = 6.74 \times 10^6\ M^{-1}$) and lifetime ($K_{SV,Tb} = 6.50 \times 10^6\ M^{-1}$) implied that dynamic quenching of the $^5D_4$ excited state of Tb^{III} was predominant in the quenching processes. The quenching rate is $k_{q,Tb} = 9.94 \times 10^9\ M^{-1}\ s^{-1}$, which was as fast as the diffusion-limited rate. Unexpectedly, the classical Tb^{III}·CAS_2 also showed luminescence quenching by 1-ethylpyridinium (D.L. $= 5.94 \times 10^{-8}$ M) and nicotinamide adenine dinucleotide (NAD, D.L. $= 2.78 \times 10^{-7}$ M). These results clearly indicate that luminescence chemosensors can be constructed not only by using covalent attachment of fluorophore to CAS and TCAS, but also in a noncovalent, supramolecular fashion.

For the remaining O,S,O sites, the formation of Ag^I_2·Tb^{III}_2·$TCAS_2$ can be regarded as such because the ternary complex utilizes the full donor sets. The formation of complex Ag^I_2·Tb^{III}_2·$TCAS_2$ was applied to the supramolecular luminescent detection of Ag^I ion at nanomolar levels [95]. As mentioned above, Ag^I_2·Tb^{III}_2·$TCAS_2$ formed at pH = 6, whereas in the absence of Ag^I ions, TCAS scarcely complexed with Tb^{III} ions. The dependence of the luminescence intensity of Ag^I_2·Tb^{III}_2·$TCAS_2$ on the Ag^I concentration was measured for $[Ag^I] = 0.5–100 \times 10^{-8}$ M with $[Tb^{III}] = 1.0 \times 10^{-6}$ M and [TCAS] $= 2.0 \times 10^{-6}$ M at pH = 6.1. The system exhibited an almost linear response to $[Ag^I]$ and yielded a D.L. of 3.2×10^{-9} M (0.35 ppb) for Ag^I at S/N = 3. Addition of fivefold amount of transition metal ions to 1.0×10^{-7} M Ag^I did not interfere except in the following cases: Cu^{II} and Fe^{III} caused negative interference due to the concomitant formation of nonluminescent Tb^{III}-TCAS ternary complex that decreased the availability of Tb^{III} ions. Cd^{II} caused a positive deviation due to the formation of the luminescent Cd^{II}_2·Tb^{III}_2·$TCAS_2$. Among halide ions, a fivefold amount of iodide caused negative interference due to its high complexation ability with Ag^I ions. Besides the analytical performance, the emergence of the function of this system should be noted (Fig. 13.12). The components Tb^{III} and TCAS do not have signaling function (i.e. luminescence) at pH = 6. However, in the presence of analyte Ag^I ions, two TCAS ligands were linked by Ag^I and coordinated to the Tb^{III} ions to form Ag^I_2·Tb^{III}_2·$TCAS_2$ to provide the signaling function as indicated by

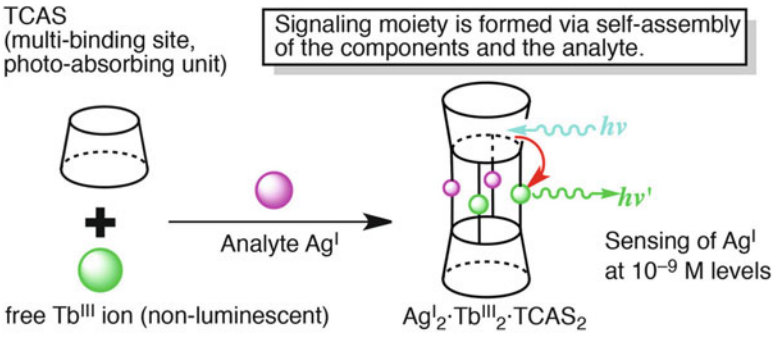

Fig. 13.12 Supramolecular sensing of Ag^{I} ion by the ternary complex formation

Eq. (13.1). Thus, this system demonstrates the supramolecular strategy to develop luminescent sensors for metal ions.

By using the self-assembly of Cd^{II}_2·Tb^{III}_2·$TCAS_2$, a determination method for nanomolar levels of Cd^{II} was developed similar to the Ag^{I} determination with the formation of Ag^{I}_2·Tb^{III}_2·$TCAS_2$ [96]. At pH 6.5 where the difference in the luminescence intensities between Cd^{II}-Tb^{III}-TCAS and Tb^{III}-TCAS systems was the largest, the calibration curve for Cd^{II} was linear to give a detection limit of ($S/N = 3$) 2.08 nM. The method was applicable to the determination of sub-ppm levels of Cd in rice, which is one of the major sources of Cd exposure. The interference by Cu^{II} and phosphate in the acid digests of rice samples were removed by masking Cu^{II} with iminodiacetate and separation of the phosphate using chelate disk, respectively. The detection limit for 1 g of a rice sample was 12.2 ppb ($S/N = 3$), which cleared the standard of cadmium in rice based on the Food Sanitation Act, Japan (0.4 ppm). Recovery for 1.007 g brown rice spiked with 3.56 nmol Cd^{II} and 2.002 g brown rice spiked with 7.12 nmol Cd^{II} were 101.0 % and 100.3 %, respectively. In addition, in the standard rice sample (certified value of Cd 0.548 ppm) measurement, result was 0.564 ppm. Thus, despite the fact that TCAS lacks the reporter group in the molecule, it was successfully applied to the practical determination of Cd^{II} by the formation of the luminescence ternary complex.

Inspired by metalloenzymes having two Lewis acid centers, and by the catalytic action of the dinuclear complex, cone-[Ti^{IV}_2(tca)Cl_4], Matsumiya devised a dinuclear complex, Ce^{IV}_2·TCAS mimicking the phosphatase enzyme [97, 98]. This complex can promote the hydrolysis of *p*-nitrophenyl phosphate with a turnover frequency of 6.8 h^{-1} at 50 °C. Moreover, the dinuclear complex can be electrostatically immobilized onto an antibody by simply mixing them together in water. The antibody labeled with the catalyst provides immunoassay of an antigen by detecting the color-development reaction (Fig. 13.13). Thus, 10 ng mL^{-1} of a tumor marker, Bence-Jones protein (BJP), in urine sample was detected by using this sensor. Here, TCAS plays an essential role not only as the ligand assembling two Ce^{IV} centers to realize the enzymatic function, but also as a platform to attach the artificial enzyme to the antibody in a noncovalent fashion.

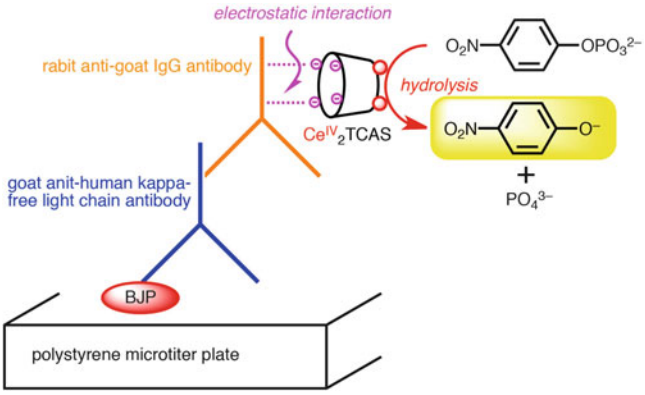

Fig. 13.13 Immunoassay for BJP using antibody labeled with Ce^{IV}-TCAS complex having hydrolysis activity

The facile conjugation of TCAS suggests the possibility of application of the diverse reporter functions of TCAS complexes, such as catalysis, energy transfer luminescence, and relaxivity, to bioanalysis and bioimaging. In combination with other components, TCAS thus provides supramolecular sensing functions, which rely on the multifunctionality of thiacalixarene.

13.5 Conclusion

As we have seen in the preceding discussion, thiacalixarene and its derivatives with oxidized sulfur bridges have unique properties and functions arising from the sulfur such as reactivity, inclusion, selective binding to the metal ions, and metal-cluster formation. Moreover, with its synergistic combination with other entities such as metal ions, profuse functions beyond prediction have emerged: separation of metal ions, Lewis acid and oxidation catalysis, giant-cage formation by self-assembly of the metal-cluster unit, molecular magnetism to lead to SMMs, energy-transfer luminescence for probes, and sensing through the formation of supramolecular metal complexes. In each case, the bridging sulfur plays an indispensable role in the emergence of the function. Some of the examples showed practical applicability, but the remaining are still on the way to the level of real situations. The supramolecular strategy to develop the function as formulated by Eq. (13.1) suggests that there is no limitation of the outcome of the function $f(x + y)$ derived from the combination of thiacalixarene x with other entity y. In addition, the number of combinations with y is unlimited, which leads to unlimited possibilities in function. To draw the nautical chart to sail the vast expanse of the thiacalix ocean, we chemists must still pursue exploratory but systematic research while expecting the discovery of novel functions.

Acknowledgements The author acknowledges with thanks Profs. S. Miyano, T. Hattori, and N. Morohashi, Tohoku University for their great suggestions, discussions, and contributions.

References

1. Sone, T.; Ohba, Y.; Moriya, K.; Kumada, H.; Ito, K. *Tetrahedron* **1997**, *53*, 10689–10698.
2. Kumagai, H.; Hasegawa, M.; Miyanari, S.; Sugawa, Y.; Sato, Y.; Hori, T.; Ueda, S.; Kamiyama, H.; Miyano, S. *Tetrahedron Lett.* **1997**, *38*, 3971–3972.
3. Gutsche, C. D. *Calixarenes*; Royal Society of Chemistry: Cambridge, 1989.
4. Iki, N.; Miyano, S. *J. Inclusion Phenom. Macrocyclic Chem.* **2001**, *41*, 99–105.
5. Morohashi, N.; Iki, N.; Miyano, S. *Yuki Gosei Kagaku Kyokaishi* **2002**, *60*, 550–562.
6. Lhoták, P. *Eur. J. Org. Chem.* **2004**, 1675–1692.
7. Morohashi, N.; Narumi, F.; Iki, N.; Hattori, T.; Miyano, S. *Chem. Rev.* **2006**, *106*, 5291–5316.
8. Iki, N. *J. Inclusion Phenom. Macrocyclic Chem.* **2009**, *64*, 1–13.
9. Iki, N. *Supramol. Chem.* **2011**, *23*, 160–168.
10. Kumar, R.; Lee, Y. O.; Bhalla, V.; Kumar, M.; Kim, J. S. *Chem. Soc. Rev.* **2014**, *43*, 4824–4870.
11. Iki, N.; Ogawa, S.; Matsue, T.; Miyano, S. *J. Electroanal. Chem.* **2007**, *610*, 90–95.
12. Iki, N.; Morohashi, N.; Suzuki, T.; Ogawa, S.; Aono, M.; Kabuto, C.; Kumagai, H.; Takeya, H.; Miyanari, S.; Miyano, S. *Tetrahedron Lett.* **2000**, *41*, 2587–2590.
13. Kondo, Y.; Ulzii, M.; Itoh, S.; Yamada, M.; Hamada, F. *Int. J. Soc. Mater. Eng. Resour.* **2014**, *20*, 103–108.
14. Morohashi, N.; Iki, N.; Aono, M.; Miyano, S. *Chem. Lett.* **2002**, *31*, 494–495.
15. Kajiwara, T.; Kon, N.; Yokozawa, S.; Ito, T.; Iki, N.; Miyano, S. *J. Am. Chem. Soc.* **2002**, *124*, 11274–11275.
16. Kajiwara, T.; Shinagawa, R.; Ito, T.; Kon, N.; Iki, N.; Miyano, S. *Bull. Chem. Soc. Jpn.* **2003**, *76*, 2267–2275.
17. Iki, N.; Kabuto, C.; Fukushima, T.; Kumagai, H.; Takeya, H.; Miyanari, S.; Miyashi, T.; Miyano, S. *Tetrahedron* **2000**, *56*, 1437–1443.
18. Patel, M. H.; Shrivastav, P. S. *Chem. Commun.* **2009**, 586–588.
19. Kundrat, O.; Eigner, V.; Dvorakova, H.; Lhoták, P. *Org. Lett.* **2011**, *13*, 4032–4035.
20. Kundrat, O.; Dvorakova, H.; Bohm, S.; Eigner, V.; Lhoták, P. *J. Org. Chem.* **2012**, *77*, 2272–2278.
21. Kundrat, O.; Dvorakova, H.; Eigner, V.; Lhoták, P. *J. Org. Chem.* **2010**, *75*, 407–411.
22. Kundrat, O.; Kroupa, J.; Bohm, S.; Budka, J.; Eigner, V.; Lhoták, P. *J. Org. Chem.* **2010**, *75*, 8372–8375.
23. Kundrat, O.; Cisarova, I.; Bohm, S.; Pojarova, M.; Lhoták, P. *J. Org. Chem.* **2009**, *74*, 4592–4596.
24. Akdas, H.; Bringel, L.; Graf, E.; Hosseini, M. W.; Mislin, G.; Pansanel, J.; De Cian, A.; Fischer, J. *Tetrahedron Lett.* **1998**, *39*, 2311–2314.
25. Morohashi, N.; Noji, S.; Nakayama, H.; Kudo, Y.; Tanaka, S.; Kabuto, C.; Hattori, T. *Org. Lett.* **2011**, *13*, 3292–3295.
26. Morohashi, N.; Miyoshi, I.; Tonosaki, A.; Ohsugi, K.; Kitamoto, Y.; Hattori, T. In *The 13th Host-Guest Chemistry Symposium, Japan* Sendai, 2015, B-16.
27. Ebata, K.; Morohashi, N.; Hattori, T. In *The 13th Host-Guest Chemistry Symposium, Japan* Sendai, 2015, 1P-12.
28. Iki, N.; Morohashi, N.; Narumi, F.; Miyano, S. *Bull. Chem. Soc. Jpn.* **1998**, *71*, 1597–1603.
29. Morohashi, N.; Iki, N.; Sugawara, A.; Miyano, S. *Tetrahedron* **2001**, *57*, 5557–5563.
30. Iki, N.; Morohashi, N.; Kabuto, C.; Miyano, S. *Chem. Lett.* **1999**, *28*, 219–220.

31. Harrowfield, J.; Koutsantonis, G. In *Calixarenes in the Nanoworld*; Vicens, J., Harrowfield, J., Baklouti, L., Eds.; Springer: Netherlands, 2007, p 197–212.
32. Kajiwara, T.; Iki, N.; Yamashita, M. *Coord. Chem. Rev.* **2007**, *251*, 1734–1746.
33. Bilyk, A.; Hall, A. K.; Harrowfield, J. M.; Hosseini, M. W.; Skelton, B. W.; White, A. H. *Inorg. Chem.* **2001**, *40*, 672–686.
34. Bilyk, A.; Dunlop, J. W.; Fuller, R. O.; Hall, A. K.; Harrowfield, J. M.; Hosseini, M. W.; Koutsantonis, G. A.; Murray, I. W.; Skelton, B. W.; Sobolev, A. N.; Stamps, R. L.; White, A. H. *Eur. J. Inorg. Chem.* **2010**, 2127–2152.
35. Bilyk, A.; Dunlop, J. W.; Fuller, R. O.; Hall, A. K.; Harrowfield, J. M.; Hosseini, M. W.; Koutsantonis, G. A.; Murray, I. W.; Skelton, B. W.; Stamps, R. L.; White, A. H. *Eur. J. Inorg. Chem.* **2010**, 2106–02126.
36. Matsumiya, H.; Iki, N.; Miyano, S.; Hiraide, M. *Anal. Bioanal. Chem.* **2004**, *379*, 867–871.
37. Matsumiya, H.; Hiraide, M. *Bull. Chem. Soc. Jpn.* **2005**, *78*, 1939–1943.
38. Matsumiya, H.; Yasuno, S.; Iki, N.; Miyano, S. *J. Chromatogr. A* **2005**, *1090*, 197–200.
39. Kikuchi, T.; Goto, I.; Suzuki, K. *J. Nucl. Sci. Technol.* **2006**, *43*, 690–693.
40. Kikuchi, T.; Suzuki, K. *J. Alloys Compd.* **2006**, *408–412*, 1287–1290.
41. Morohashi, N.; Hattori, T.; Yokomakura, K.; Kabuto, C.; Miyano, S. *Tetrahedron Lett.* **2002**, *43*, 7769–7772.
42. Morohashi, N.; Yokomakura, K.; Hattori, T.; Miyano, S. *Tetrahedron Lett.* **2006**, *47*, 1157–1161.
43. Proto, A.; Giugliano, F.; Capacchione, C. *Eur. Polym. J.* **2009**, *45*, 2138–2141.
44. Floriani, C.; Floriani-Moro, R. In *Calixarenes 2001*; Kluwer Academic Publishers: 2001, p 536–560.
45. Yilmaz, M. In *Calixarenes and Beyond*; Neri, P., Ed.; Springer: 2016.
46. Limberg, C. *Eur. J. Inorg. Chem.* **2007**, 3303–3314.
47. Su, K.; Jiang, F.; Qian, J.; Gai, Y.; Wu, M.; Bawaked, S. M.; Mokhtar, M.; Al-Thabaiti, S. A.; Hong, M. *Cryst. Growth Des.* **2014**, *14*, 3116–3123.
48. Su, K.; Jiang, F.; Qian, J.; Pang, J.; Al-Thabaiti, S. A.; Bawaked, S. M.; Mokhtar, M.; Chen, Q.; Hong, M. *Cryst. Growth Des.* **2014**, *14*, 5865–5870.
49. Bi, Y.; Wang, X.-T.; Liao, W.; Wang, X.; Wang, X.; Zhang, H.; Gao, S. *J. Am. Chem. Soc.* **2009**, *131*, 11650–11651.
50. Gehin, A.; Ferlay, S.; Harrowfield, J. M.; Fenske, D.; Kyritsakas, N.; Hosseini, M. W. *Inorg. Chem.* **2012**, *51*, 5481–5486.
51. Bi, Y.; Du, S.; Liao, W. *Chem. Commun.* **2011**, *47*, 4724–4726.
52. Bi, Y.; Du, S.; Liao, W. *Coord. Chem. Rev.* **2014**, *276*, 61–72.
53. Bi, Y.; Xu, G.; Liao, W.; Du, S.; Wang, X.; Deng, R.; Zhang, H.; Gao, S. *Chem. Commun.* **2010**, *46*, 6362–6364.
54. Xiong, K.; Jiang, F.; Gai, Y.; He, Z.; Yuan, D.; Chen, L.; Su, K.; Hong, M. *Cryst. Growth Des.* **2012**, *12*, 3335–3341.
55. Bi, Y.; Wang, S.; Liu, M.; Du, S.; Liao, W. *Chem. Commun.* **2013**, *49*, 6785–6787.
56. Du, S.; Yu, T.-Q.; Liao, W.; Hu, C. *Dalton Trans.* **2015**, *44*, 14394–14402.
57. Dai, F.-R.; Wang, Z. *J. Am. Chem. Soc.* **2012**, *134*, 8002–8005.
58. Dai, F.-R.; Becht, D. C.; Wang, Z. *Chem. Commun.* **2014**, *50*, 5385–5387.
59. Dai, F.-R.; Sambasivam, U.; Hammerstrom, A. J.; Wang, Z. *J. Am. Chem. Soc.* **2014**, *136*, 7480–7491.
60. Kajiwara, T.; Hasegawa, M.; Ishii, A.; Katagiri, K.; Baatar, M.; Takaishi, S.; Iki, N.; Yamashita, M. *Eur J Inorg Chem* **2008**, 5565–5568.
61. Bi, Y.; Wang, X.-T.; Liao, W.; Wang, X.; Deng, R.; Zhang, H.; Gao, S. *Inorg. Chem.* **2009**, *48*, 11743–11747.
62. Desroches, C.; Pilet, G.; Borshch, S. A.; Parola, S.; Luneau, D. *Inorg. Chem.* **2005**, *44*, 9112–9120.
63. Desroches, C.; Pilet, G.; Szilagyi, P. A.; Molnar, G.; Borshch, S. A.; Bousseksou, A.; Parola, S.; Luneau, D. *Eur. J. Inorg. Chem.* **2006**, 357–365.

64. Lamouchi, M.; Jeanneau, E.; Novitchi, G.; Luneau, D.; Brioude, A.; Desroches, C. *Inorg. Chem.* **2014**, *53*, 63–72.
65. Xiong, K.; Wang, X.; Jiang, F.; Gai, Y.; Xu, W.; Su, K.; Li, X.; Yuan, D.; Hong, M. *Chem. Commun.* **2012**, *48*, 7456–7458.
66. Su, K.; Jiang, F.; Qian, J.; Wu, M.; Xiong, K.; Gai, Y.; Hong, M. *Inorg. Chem.* **2013**, *52*, 3780–3786.
67. Eliseeva, S. V.; Bünzli, J. C. *Chem. Soc. Rev.* **2010**, *39*, 189–227.
68. Eliseeva, S. V.; Bünzli, J.-C. G. *New J. Chem.* **2011**, *35*, 1165–1176.
69. Zhu, X.-H.; Peng, J.; Cao, Y.; Roncali, J. *Chem. Soc. Rev.* **2011**, *40*, 3509–3524.
70. Liu, Z.; Zhang, G.; Zhang, D. *Chem. – Eur. J.* **2016**, *22*, 462–471.
71. Sabbatini, N.; Guardigli, M.; Manet, I.; Ziessel, R. In *Calixarenes 2001*; Kluwer Academic Publishers: 2001, p 583–597.
72. Iki, N.; Horiuchi, T.; Oka, H.; Koyama, K.; Morohashi, N.; Kabuto, C.; Miyano, S. *J. Chem. Soc. Perkin Trans.* **2001**, *2*, 2219–2225.
73. Matsumiya, H.; Masai, H.; Terazono, Y.; Iki, N.; Miyano, S. *Bull. Chem. Soc. Jpn.* **2003**, *76*, 133–136.
74. Iki, N.; Ohta, M.; Horiuchi, T.; Hoshino, H. *Chem. – Asian J.* **2008**, *3*, 849–853.
75. Tanaka, T.; Iki, N.; Kajiwara, T.; Yamashita, M.; Hoshino, H. *J. Inclusion Phenom. Macrocyclic Chem.* **2009**, *64*, 379–383.
76. Iki, N.; Hiro-oka, S.; Tanaka, T.; Kabuto, C.; Hoshino, H. *Inorg. Chem.* **2012**, *51*, 1648–1656.
77. Iki, N.; Tanaka, T.; Hoshino, H. *Inorg. Chim. Acta* **2013**, *397*, 42–47.
78. Bünzli, J.-C. G. *J. Lumin.* **2016**, *170*, 866–878.
79. Iki, N.; Hiro-oka, S.; Nakamura, M.; Tanaka, T.; Hoshino, H. *Eur. J. Inorg. Chem.* **2012**, 3541–3545.
80. Iki, N.; Boros, E.; Nakamura, M.; Baba, R.; Caravan, P. *Inorg. Chem.* **2016**, *55*, 4000–4005.
81. Karashimada, R.; Iki, N. *Chem. Commun.* **2016**, *52*, 3139–3142.
82. Tang, W.; Su, M. *Appl. Mech. Mater.* **2014**, *687–691*, 4223–4227.
83. Song, M.; Sun, Z.; Han, C.; Tian, D.; Li, H.; Kim, J. S. *Chem. – Asian J.* **2014**, *9*, 2344–2357.
84. Patra, S.; Maity, D.; Gunupuru, R.; Agnihotri, P.; Paul, P. *J. Chem. Sci.* **2012**, *124*, 1287–1299.
85. Kim, H. N.; Ren, W. X.; Kim, J. S.; Yoon, J. *Chem. Soc. Rev.* **2012**, *41*, 3210–3244.
86. Sharma, K.; Cragg, P. J. *Chem. Sens.* **2011**, *1*, 1–18.
87. Ben Ali, M.; Bureau, C.; Martelet, C.; Jaffrezic-Renault, N.; Lamartine, R.; Ben Ouada, H. *Mater. Sci. Eng., C* **2000**, *C7*, 83–89.
88. Ben Ali, M.; Jaffrezic-Renault, N.; Martelet, C.; Ben Ouada, H.; Davenas, J.; Charbonnier, M. *Mater. Sci. Eng., C* **2001**, *C14*, 17–23.
89. Zheng, H.; Yan, Z.; Dong, H.; Ye, B. *Sens. Actuators, B* **2007**, *120*, 603–609.
90. Wang, L.; Wang, X.; Shi, G.; Peng, C.; Ding, Y. *Anal. Chem.* **2012**, *84*, 10560–10567.
91. Jin, T.; Fujii, F.; Yamada, E.; Nodasaka, Y.; Kinjo, M. *Comb. Chem. High Throughput Screen.* **2007**, *10*, 473–479.
92. Hu, X.-J.; Li, C.-M.; Song, X.-Y.; Zhang, D.; Li, Y.-S. *Inorg. Chem. Commun.* **2011**, *14*, 1632–1635.
93. Horiuchi, T.; Iki, N.; Oka, H.; Miyano, S. *Bull. Chem. Soc. Jpn.* **2002**, *75*, 2615–2619.
94. Horiuchi, T.; Iki, N.; Hoshino, H. *Anal. Chim. Acta* **2009**, *650*, 258–263.
95. Iki, N.; Ohta, M.; Tanaka, T.; Horiuchi, T.; Hoshino, H. *New J. Chem.* **2009**, *33*, 23–25.
96. Abe, N.; Hoshino, H.; Iki, N. *Bunseki Kagaku* **2015**, *64*, 493–499.
97. Matsumiya, H.; Nakamura, H.; Hiraide, M. *Anal. Bioanal. Chem.* **2009**, *394*, 1471–1476.
98. Nagai, S.; Matsumiya, H.; Hiraide, M. *Bunseki Kagaku* **2012**, *61*, 723–726.